JOURNAL OF SOLID STATE CHEMISTRY 59, 362–370 (1985)

Intergrowth Phases in the Fe_9PO_{12}–Fe_7SiO_{10} System

C. GLEITZER AND A. MODARESSI

Laboratoire de Chimie du Solide Mineral, Université de Nancy 1, Boite Postale 239, 54506 Vandoeuvre les Nancy Cedex, France

AND R. J. D. TILLEY

Department of Metallurgy and Materials Science, University College, Newport Road, Cardiff CF2 1TA, Great Britain

Received November 28, 1984; in revised form March 11, 1985

A series of samples spanning the composition range between the phases Fe_9PO_{12} and Fe_7SiO_{10} have been prepared at 1173 K. These have been studied by powder X-ray diffraction and transmission electron microscopy. This latter technique revealed that over the middle part of the composition range intergrowth between unit cell thickness slabs of the two end-member phases occurred. These intergrowths were sometimes disordered but ordered regions also occurred showing that a set of microphases can form in this system. Apart from stacking disorder the electron diffraction patterns often revealed continuous lines of diffuse scattering as well as the normal sharp diffraction spots. This was found all across the composition range including the end-member phases and is believed to be due to disorder among the cations present.

Introduction

Some years ago an iron silicate was isolated in material taken from the floor of a reheating furnace. The subsequent X-ray structure determination combined with chemical analysis yielded a formula Fe_7SiO_{10}. The unit cell was found to be monoclinic, with $a = 2.14$ nm, $b = 0.306$ nm, $c = 0.588$ nm, $\beta = 98°$ (*1*). The structure was described as being built up from slabs of composition FeO which are linked by lamellae of composition Fe_3SiO_6. The FeO lamellae have the rock-salt structure and can be considered to be thin slabs of wüstite. This is illustrated schematically in Fig. 1a.

More recently, during an extensive study of the Fe–P–O system, an oxyphosphate of composition Fe_9PO_{12} was isolated. The orthorhombic unit cell has dimensions $a = 0.595$ nm, $b = 0.3065$ nm, $c = 2.57$ nm. This phase proved to have a structure rather similar to that of Fe_7SiO_{10} in that it was also built up from wüstite slabs. In this compound, though, they were linked by lamellae of composition Fe_3PO_6 (*2*). The structure is illustrated schematically in Fig. 1b. In this material we believe that the valence of the P atoms should be taken as 5+. This is because P^{5+} seems to be stable in the presence of Fe^{2+}, as shown, for instance, by $Fe_2P_2O_7$ (*8*), and in the presence of Fe^{3+}, as shown by $Fe_3(PO_4)_2$ (*9*). Hence, in Fe_9PO_{12} it seems reasonable to take the valence of the P atoms as 5+ and distribute

0022-4596/85 $3.00

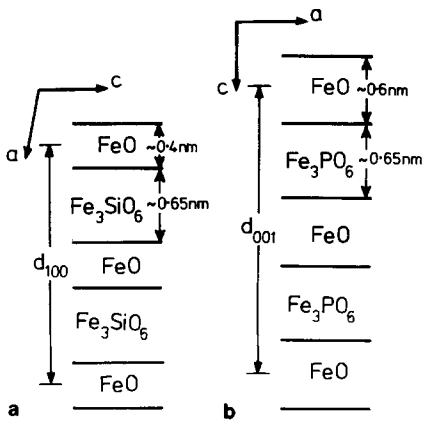

FIG. 1. Schematic illustration of the structures of (a) Fe_7SiO_{10} and (b) Fe_9PO_{12}. Both structures are composed of alternating slabs of FeO and Fe_3MO_6, where M is either Si or P.

the charges on the Fe atoms, 2+ and 3+, to fulfill compositional requirements.

The similarity between these two structures is marked, and suggested that compositions intermediate between the two parent phases, Fe_7SiO_{10} and Fe_9PO_{12}, might be accommodated by structural intergrowth. As no work has been reported in this composition region that would allow this speculation to be checked, experiments were carried out to explore the possibility further. These are reported in this publication.

Experimental

The samples examined were prepared by heating mixtures of SiO_2, Fe, and Fe_2O_3 or Fe_2SiO_4, Fe, and Fe_2O_3 for Fe_7SiO_{10}; $FePO_4$, Fe, and Fe_2O_3 for Fe_9PO_{12}, and SiO_2, $FePO_4$, Fe, and Fe_2O_3 or Fe_2SiO_4, $FePO_4$, Fe, and Fe_2O_3 for intermediate compositions. The mixtures were sealed in evacuated sealed silica ampoules and heated for several days at temperatures close to 1200 K, as detailed in Table I. Some of the preparations were recrystallized by resealing them in evacuated silica ampoules together with a trace of $FeCl_2$ which acts as a mineralizer and transporting agent. These were then heated for several days at the same temperature as the initial preparation. After heat treatment, all samples were rapidly air-cooled.

All samples were examined by powder X-ray diffraction using a Guinier camera of

TABLE I

SAMPLES EXAMINED AND X-RAY POWDER DIFFRACTION PHASE ANALYSIS

Sample no.	Sample gross composition	Preparation conditions: Heating time, days	Preparation conditions: Temperature, K	X-Ray powder diffraction phase analysis
17	$Fe_9(PO_4)O_8$	3	1200	Fe_9PO_{12}
16	$Fe_9(P_{0.75}Si_{0.25}O_4)O_8$	3	1200	Fe_9PO_{12}
27 R[a]	$Fe_9(P_{0.75}Si_{0.25}O_4)O_8$	5	1200	Fe_9PO_{12}
11 R	$Fe_7(P_{0.5}Si_{0.5}O_4)O_6$	3	1203	Fe_7SiO_{10}
26	$Fe_9(P_{0.5}Si_{0.5}O_4)O_8$	5	1203	Fe_9PO_{12}
24 R	$Fe_7(P_{0.5}Si_{0.5}O_4)O_6$	8	1203	Fe_7SiO_{10}
19	$Fe_7(P_{0.5}Si_{0.5}O_4)O_6$	1	1273	Fe_7SiO_{10}
22 R	$Fe_7(Si_{0.75}P_{0.25}O_4)O_6$	7	1203	Fe_7SiO_{10}
12	$Fe_7(SiO_4)O_6$	5	1208	Fe_7SiO_{10} + Fe_3O_4 + $Fe_{1-x}O$[b]
23 R	Fe_7SiO_{10}	11	1208	Fe_7SiO_{10} + Fe_3O_4 + $Fe_{1-x}O$[b]

[a] R indicates that the original preparation recrystallized.

[b] The composition of the nonstoichiometric wüstite phase was not determined in these samples.

Seeman-Bohlin pattern and Co$K\alpha$ radiation.

For electron microscope analysis, crystals were crushed in an agate mortar under *n*-butanol. A drop of the resultant suspension was allowed to dry on a net-like carbon film on a copper support grid. Crystal fragments projecting over holes in the carbon film were examined in detail using a Jeol JEM 200 electron microscope fitted with a rotation/tilt stage which allowed samples to be tilted through ±60°. "Lattice fringe" images were taken at the top magnification of 330,000×, using (00*l*) systematic reflections and a total of 13 beams (including 000) for Fe_9PO_{12} and (*h*00) systematic reflections and 11 beams (including 000) for Fe_7SiO_{10}.

Results

The phase Fe_7SiO_{10} has not been deliberately synthesized before, as the material which was the subject of the original crystal structure determination was extracted from a furnace residue. Some difficulty was found in preparing the compound, as can be seen from Table I. In fact complete reaction was difficult to obtain and nonnegligible quantities of Fe_2SiO_4, FeO, and Fe_3O_4 were also present in preparations. In contradiction to this, however, the preparations containing even small amounts of P were more reactive and gross amounts of impurities were not found in the reaction products.

Electron Microscope Phase Analysis

For phase analysis, the long unit cell axis is the most important characteristic of these materials while the other two axes, being similar in the two structures, do not give unequivocal data. Hence all crystal fragments were oriented so that the long axis was aligned perpendicular to the electron beam. Thus, reciprocal lattice sections were sought which contained the c^* axis of Fe_9PO_{12} (c = 2.57 nm) and the a^* axis of Fe_7SiO_{10} (a = 2.14 nm).

The results obtained showed that for Fe_9PO_{12}, the reflections present along 00*l* were those with *l* even (i.e., 002, 004, etc.) and for Fe_7SiO_{10} the reflections present along *h*00 were those with *h* even (i.e., 200, 400, etc.). Figure 2 shows examples of these patterns. The measured values of a and c derived from these diffraction patterns were in agreement with the X-ray data. No other long periodicities were found on any diffraction patterns, apart from the intergrowth phases described below. Hence, all crystal fragments examined could be assigned to Fe_9PO_{12} or Fe_7SiO_{10}.

In samples with compositions between Fe_9PO_{12} and $Fe_9P_{0.75}Si_{0.25}O_{12}$ the vast majority of crystal fragments were of the Fe_9PO_{12} type, but a few did have the Fe_7SiO_{10} unit cell. In samples of composition $Fe_9P_{0.5}Si_{0.5}O_{12}$, more fragments were of the Fe_7SiO_{10} type than of the Fe_9PO_{12} type, but the relative numbers of each sort varied from sam-

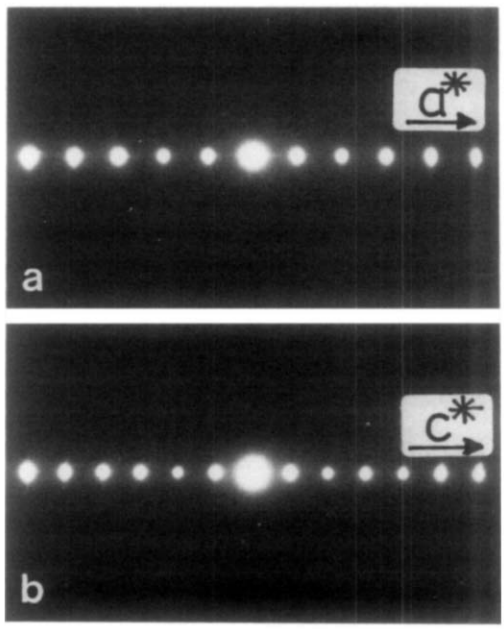

FIG. 2. Diffraction patterns from (a) the (*h*00) row of Fe_7SiO_{10} and (b) the (00*l*) row of Fe_9PO_{12}. The extent of these figures shows the number of reflections contributing to the images in micrographs.

ple to sample. This reflects the weakness of electron microscopy for phase analysis of this sort as well as any sample inhomogeneity present. In samples of composition lying between Fe_7SiO_{10} and $Fe_9P_{0.25}Si_{0.75}O_{12}$, all but one of the crystal fragments examined were of the Fe_7SiO_{10} type, the exception being a coherent intergrowth of large regions of the Fe_9PO_{12} and Fe_7SiO_{10} crystal types. In addition, some fragments of Fe_2SiO_4 were also found in Fe_7SiO_{10} preparation.

At the level of discrimination provided by the analysis, the region is a two-phase one, with Fe_9PO_{12} and Fe_7SiO_{10} being present. The question of whether a solid-solution range exists at either end of the phase range is not directly answered by these results. However, as in the composition range Fe_7SiO_{10}–$Fe_9P_{0.25}Si_{0.75}O_{12}$, no pure crystals were found with an axial spacing corresponding to Fe_9PO_{12}, it suggests that Fe_7SiO_{10} is able to take Fe_9PO_{12} (or P) into solid solution. At the other end of the range, in the samples of $Fe_9P_{0.75}Si_{0.25}O_{12}$ examined of the 22 crystals studied, 20 were of the $Fe_9P_{0.75}Si_{0.25}O_{12}$ type and 2 possessed the Fe_7SiO_{10} ($h00$) spacing. This suggests that some solid solution of Fe_7SiO_{10} in Fe_9PO_{12} may take place, but the limit is lower than at the other end of the phase range.

Microstructures

The microstructures of the crystals examined were imaged by using a total of 13 beams for Fe_9PO_{12} and 11 beams for Fe_7SiO_{10}. The systematic $h00$ or $00l$ rows were used, and the micrographs therefore contain only one-dimensional fringes, with a spacing corresponding to (200) for Fe_7SiO_{10} and to (002) for Fe_9PO_{12}. The information in the images is therefore rather limited. It does, however, reveal if intergrowths or similar defects occur.

The end members of the series, Fe_9PO_{12} and Fe_7SiO_{10}, were well ordered, and no obvious faulting was found. In all of the other compositions examined faulted crystal fragments were sometimes observed, as well as well-ordered crystal fragments. The faults took the form of lamellae of thickness corresponding to one of the end members in a matrix predominantly of the other member. These faults were sometimes isolated and sometimes clustered. In some crystal fragments the density of the faults was very high, and the crystal fragments themselves were very disordered. Typical examples are shown in Fig. 3.

Occasionally some crystal fragments were found in which the faults were ordered or quasiordered. In the present investigation, this has only been found so far in crystal fragments taken from samples of overall composition $Fe_9P_{0.5}Si_{0.5}O_{12}$ and then only in fragments in which the matrix or major component has corresponded to an Fe_7SiO_{10} unit cell.

In these ordered crystals, several slabs of Fe_7SiO_{10}-type separate single lamellae of Fe_9PO_{12}, as is illustrated in Fig. 4. To date two well-ordered patterns have been found, corresponding to 3 units of Fe_7SiO_{10} to 1 unit of Fe_9PO_{12} (Fig. 4a) and to 4 units of Fe_7SiO_{10} to 1 unit of Fe_9PO_{12} (Fig. 4b). A number of other ordering patterns have also been found which are not quite perfect but which show larger repeat distances. One of these is also shown in Fig. 4c. No ordered examples were found where the lamellae of Fe_9PO_{12} were thicker than d_{200}, or where isolated lamellae of Fe_7SiO_{10} ordered in a Fe_9PO_{12} matrix.

Diffuse Intensity

The presence of planar faults or disordered intergrowth, as described above, gives rise to streaks on electron diffraction patterns. These streaks pass through *every* normally allowed reflection and the direction of the streaks is parallel to the reciprocal lattice direction which is normal to the fault plane (*4*). Hence, for Fe_9PO_{12}, the

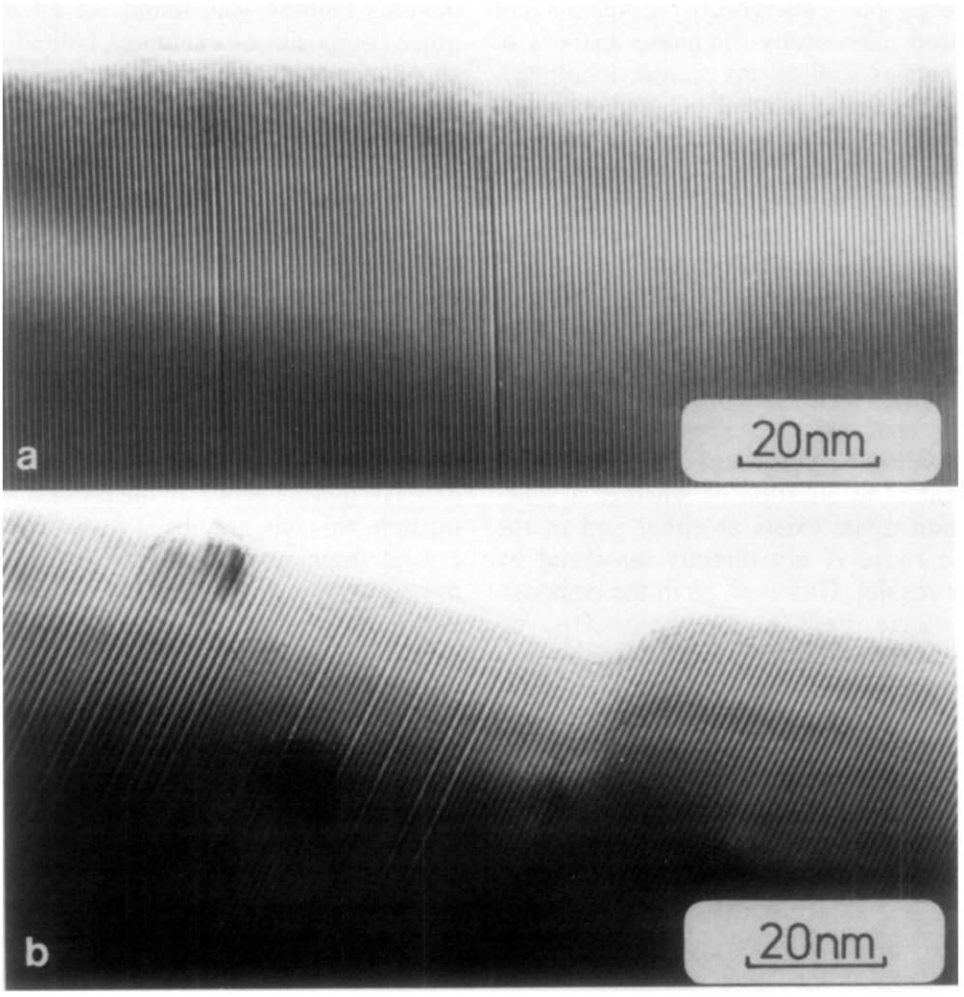

FIG. 3. Electron micrographs showing disordered intergrowth between Fe_7SiO_{10} and Fe_9PO_{12}. (a) Two isolated lamella of Fe_9PO_{12} type in a matrix of Fe_7SiO_{10} type. (b) A number of disordered lamellae of Fe_9PO_{12} type in a matrix of Fe_7SiO_{10} type together with a thin region of Fe_9PO_{12} type at the left. In both micrographs the intergrowths are most easily visible in the thicker parts of the crystal, but the true lamellae thicknesses are only accurately revealed at the crystal edge.

streaks run parallel to c^*, which is parallel to g_{002} and normal to the (002) planes. In Fe_7SiO_{10} the streaks run parallel to a^*, i.e., parallel to g_{200}, which is normal to the (200) planes.

In the materials examined, an additional diffuse intensity was observed. This took the form of continuous lines, sometimes not associated with any normal lattice reflections, sometimes running along rows of reflections. The direction of these lines was always parallel to a^* for Fe_7SiO_{10} and to c^* for Fe_9PO_{12}, that is, they were normal to the slabs which make up the structure. Examples are shown on Fig. 5. The diffuse scattering is not due to the intergrowth faults, because, as stated, intergrowth will cause all normal spots to be streaked. However, in addition, these diffuse lines of intensity were observed in the *pure* end mem-

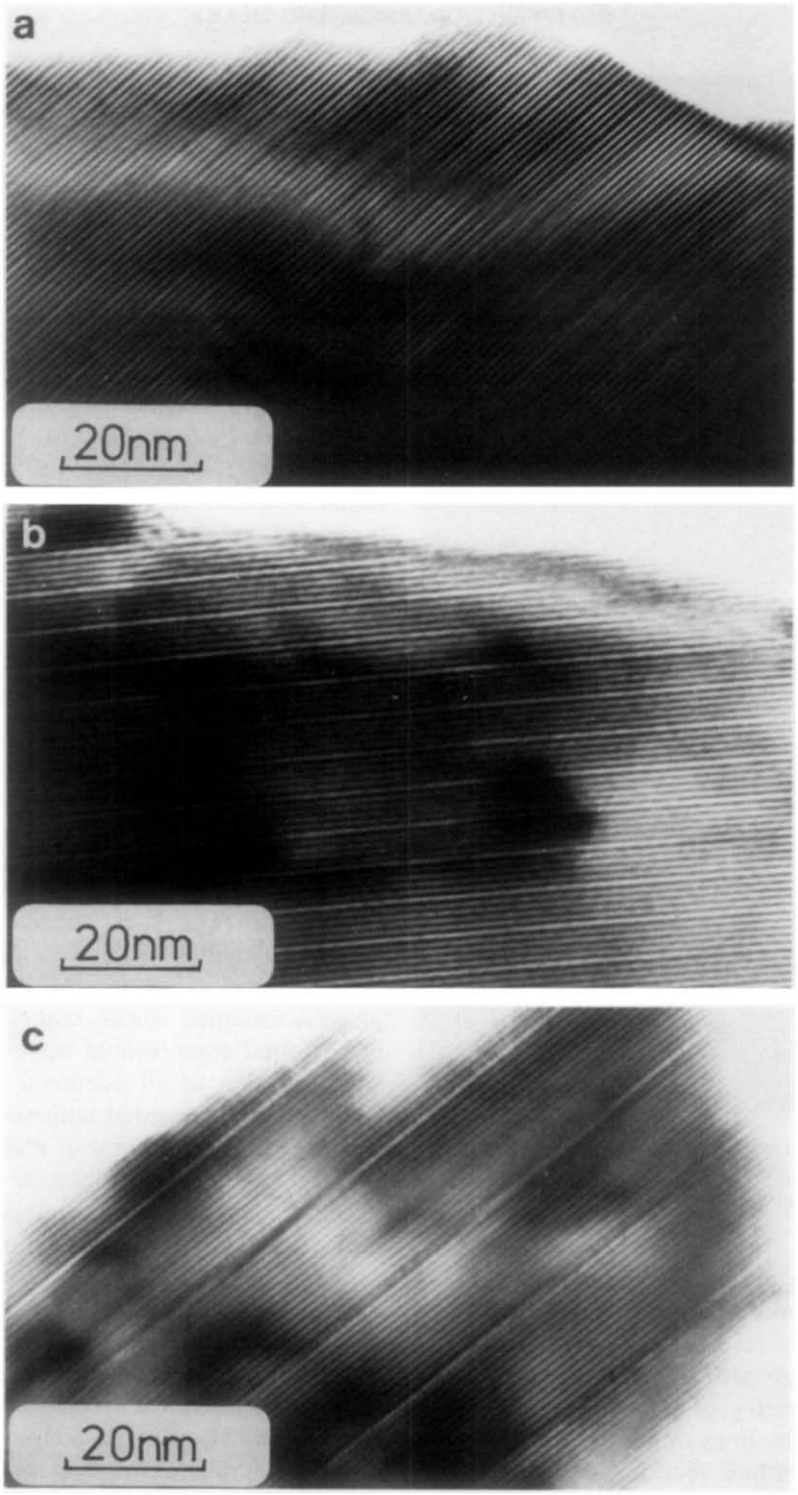

FIG. 4. Electron micrographs of crystals containing well-ordered intergrowths between lamellae of Fe_7SiO_{10} and Fe_9PO_{12} types. (a) Sequence of 3 lamellae of Fe_7SiO_{10} type followed by one of Fe_9PO_{12} type; (b) sequence of 4 lamellae of Fe_7SiO_{10} type followed by one of Fe_9PO_{12} type; (c) sequence of approximately 14 lamellae of Fe_7SiO_{10} type followed by one of Fe_9PO_{12} type.

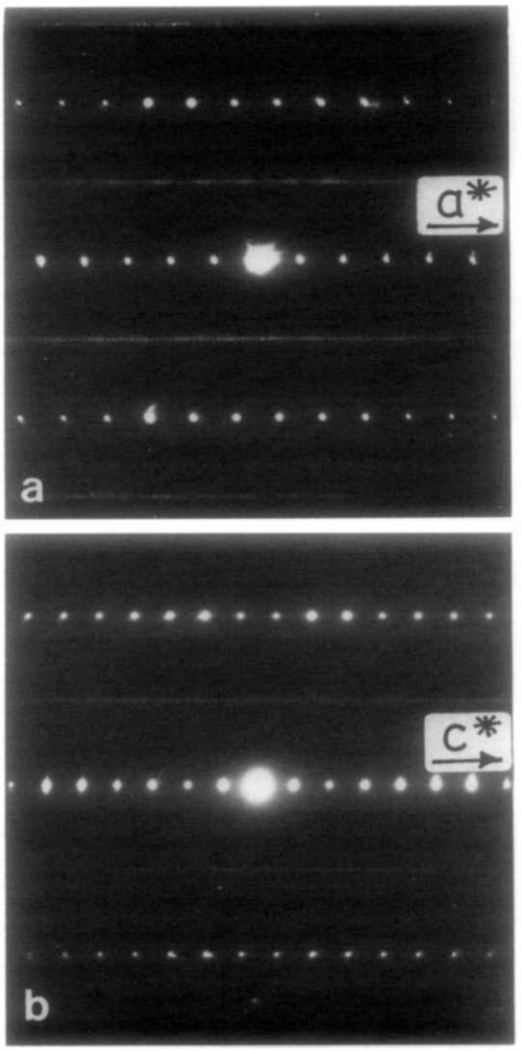

FIG. 5. Electron diffraction patterns of (a) Fe_7SiO_{10} and (b) Fe_9PO_{12} showing diffuse lines of intensity, parallel to a^* in (a) and c^* in (b).

bers of the series Fe_9PO_{12} and Fe_7SiO_{10}, which showed no intergrowth faulting, and in other crystal fragments which showed perfect fringe patterns with no disorder.

The geometry of the streaking is quite complex. The lines do not appear on every reciprocal lattice section, and in order to check whether any particular diffraction pattern showed diffuse lines of intensity it was necessary to tilt crystals over as wide a range of angles as possible. As it was not always possible to tilt crystals very far it is not certain whether all diffraction patterns show diffuse scattering or whether some contain only sharp spots.

Discussion

The electron microscope phase analysis shows that over the phase range studied only two unit cells occur, corresponding to Fe_9PO_{12} and Fe_7SiO_{10}. Over the greater part of the phase range, faulted crystals are found in which the matrix of one structure type contains lamellae of the other structure. These lamellae are often disordered, but sometimes ordered, and in this case a set of discrete microphases is formed.

This result suggests that an extensive solid solution between the two phases does not exist under all preparation conditions. Instead, when sufficient Si is present in what is effectively the Fe_9PO_{12} phase a lamella of Fe_7SiO_{10} type is laid down and whenever sufficient P is present in a matrix of Fe_7SiO_{10} a lamella of Fe_9PO_{12} is laid down. The results do suggest, however, that some solid solution may take place in the composition region close to the parent phases, because fewer faulted fragments were found than should have been if no solid solution at all occurred. This statement must be regarded with some caution, however, as the amount of material examined by transmission electron microscopy is small, and can be unrepresentative of bulk phase composition. A more accurate assessment of solid-solution formation can hence be gained from X-ray powder diffraction and other phase analysis techniques.

All across the phase range examined, crystal fragments corresponding to unfaulted Fe_9PO_{12} and Fe_7SiO_{10} were found, as well as disordered and ordered intergrowth. This behavior suggests that the preparations may have been made at a temperature close to a phase boundary such

that below the temperature only Fe_7SiO_{10} and Fe_9PO_{12} coexist, while above it intergrowth phases occur. A similar situation has been found in the TiO_2–Ga_2O_3 system for example, where, below approximately 1473 K TiO_2 coexists with $TiGa_2O_5$, while above this temperature a complex series of intergrowth phases form (*5*). By drawing parallels it may be that preparations carried out at higher temperatures in the Fe_9PO_{12}–Fe_7SiO_{10} system would yield a more extensive series of ordered phases, while preparations at lower temperatures would lead to two-phase coexistence between Fe_9PO_{12} and Fe_7SiO_{10}. Such studies are planned for the future, although the high-temperature stability of the parent compounds makes experiments at significantly higher temperatures than those already employed very difficult.

Although the electron micrographs show beyond doubt that intergrowths exist, we cannot, at the moment give precise structures or formulae. The problem is associated with the structure proposed for iscorite, Fe_7SiO_{10}. A parallel study by X-ray diffraction, shows that a more correct formula for the phase may be closer to $Fe_{7.06}Si_{0.94}O_{10}$ (*6*). In this case, some silicon is replaced by Fe^{3+} and a cation vacancy, to maintain charge neutrality. However, if we take the idealized formulae of the intergrowth parent phases to be those given by the crystal structures already published we can write idealized formulae. In Fe_7SiO_{10}, there are two formula units per unit cell, and hence one (Fe_7SiO_{10}) per slab imaged in the micrographs. In the case of Fe_9PO_{12}, the unit cell contains two formula units, and each slab imaged in the micrographs will contain one (Fe_9PO_{12}). As the phases found so far have isolated slabs of Fe_9PO_{12}, the series formula is then $Fe_9PO_{12} \cdot n(Fe_7SiO_{10})$, with n taking values of 3 and 4. Clearly the real structures of these compounds may differ from this idealized situation, as the interface region between the FeO slabs may be considerably modified from that existing in the parent compounds. Further considerations should therefore be postponed until high-resolution electron microscope studies have been completed. At this time, the structure of the intergrowths and of Fe_7SiO_{10} cannot be discussed in detail.

One of the more interesting results of this investigation is the observation of diffuse streaking on the diffraction patterns. The diffuse streaking noted is not due to the intergrowth phenomenon as it is also found on diffraction patterns of the end-member phases, Fe_9PO_{12} and Fe_7SiO_{10}. As the matrix reflections are not affected it is also clear that much of the structure is perfect and only one part of it is disordered from a structural point of view.

Lines of diffusion scattering can arise in a number of ways. Very similar diffraction effects are found in a lattice in which we have an alternation of two atom species in a direction normal to the streaking, and a random distribution of the two species in the direction of the streaking (*7*). The most likely contenders for the disordered atomic species are Fe and P in the Fe_3PO_6 lamellae and Fe and Si in the $FeSiO_4$ lamellae. If the structures of Fe_7SiO_{10} and Fe_9PO_{12} are examined, it is found that the Si^{4+} and Fe^{3+} or P^{5+} and Fe^{3+} occupy similar sites in the planes between the FeO blocks. Clearly, if the Si^{4+} and Fe^{3+} or P^{5+} and Fe^{3+} are able to exchange positions, or if the position that each atom occupies during crystal growth is rather flexible, then there is the possibility that the alternation needed can arise. If there is no or little correlation between the sheets containing the alternating atoms then diffuse lines of intensity would arise, between normal reciprocal lattice rows. At this point of the investigation it is impossible to be more precise, but high-resolution electron micrography and theoretical studies now underway may be able to clarify this further.

Acknowledgments

R. J. D. Tilley is grateful to Dr. C. Gleitzer and Professor B. Roques for support which made the research described here possible.

References

1. J. SMUTS, J. STEYN, AND J. BOEYENS, *Acta Crystallogr. Sect. B* **25,** 1251 (1969).
2. G. VENTURINI, A. COURTOIS, J. STEINMETZ, R. GERARDIN, AND G. GLEITZER, *J. Solid State Chem.* **53,** 1 (1984).
3. J. G. ALLPRESS AND J. A. SANDERS, *J. Appl. Crystallogr.* **6,** 165 (1973).
4. P. B. HIRSCH, A. HOWIE, R. B. NICHOLSON, D. W. PASHLEY, AND M. J. WHELAN, "Electron Microscopy of Thin Crystals," Butterworths, London (1965).
5. S. KAMIYA AND R. J. D. TILLEY, *J. Solid State Chem.* **22,** 205 (1977).
6. A. MODARESSI, B. MALAMAN, C. GLEITZER, AND R. J. D. TILLEY, submitted for publication.
7. G. HARBURN, C. A. TAYLOR, AND T. R. WELBERRY, "Atlas of Optical Transforms," Plate 18, Bell, London (1975).
8. J. HOGGINS, H. SWINNEA, AND H. STEINFINK, *J. Solid State Chem.* **47,** 278 (1983).
9. E. KOSTINER AND J. REA, *Inorg. Chem.* **13,** 2876 (1974).